

KfK 2820  
Juli 1979

# **Observations of the Behaviour of Gas in the Wake behind a Corner Blockage in Fast Breeder Reactor Subassembly Geometry**

Y. Fukuzawa  
Institut für Reaktorentwicklung  
Projekt Schneller Brüter

**Kernforschungszentrum Karlsruhe**



KERNFORSCHUNGSZENTRUM KARLSRUHE  
Institut für Reaktorentwicklung  
Projekt Schneller Brüter

KfK 2820

Observations of the Behaviour of Gas in the Wake  
behind a Corner Blockage in Fast Breeder Reactor  
Subassembly Geometry

Y. Fukuzawa

Als Manuskript vervielfältigt  
Für diesen Bericht behalten wir uns alle Rechte vor

Kernforschungszentrum Karlsruhe GmbH  
ISSN 0303-4003

## Abstract

Observations were made of gas behaviour in the wake behind a 21 % corner blockage in the subassembly geometry of a liquid metal fast breeder reactor. The test section used represented one half of the reactor fuel subassembly, divided along the vertical plane of symmetry through the blockage. A glass wall occupied the position of this plane. Water was allowed to flow between glass rods simulating fuel pins, the velocity being changed from 1.2 to 4.5 m/s. Argon was injected into the wake or into the flow upstream of the blockage, the injection rate being changed from 1 to 230 Ncm<sup>3</sup>/s (standard temperature and pressure).

From the present experiment, the following is evident: The gas is accumulated in the wake behind the blockage, forming a gas cavity. The flow patterns of the two-phase mixture in the wake are classified into three types, depending on the liquid velocity. In the lower velocity range, a gas cavity cannot be present at rest, rising up through the wake as a single bubble due to buoyancy. In the higher velocity range, the gas cavity is broken up by the liquid flow forces, only small gas bubbles circulating in the wake. In the velocity range in between, the gas cavity is present in the wake. The cavity size depends on the gas injection rate and on the liquid velocity.

From the results, the possibility of fuel failure caused by fission gas release at a blockage in the fast breeder reactor can be considered to depend on the operating conditions of the reactor, specially on the coolant velocity.

## Zusammenfassung

Beobachtungen zum Verhalten des Gases in der Rückströmung hinter einer Randblockade in einer Brennelement-Anordnung ähnlich einem Schnell-Brüter-Brennelement

---

Das Verhalten von Gasblasen im Totwassergebiet hinter einer 21 %-Eckblockade in einem Brennelement des schnellen natriumgekühlten Brutreaktors wurde mit einem simulierten Brennelement in einem Wasserkreislauf untersucht.

Die verwendete Versuchseinrichtung repräsentierte die Hälfte eines Brennelements, wobei die Schnittebene entlang der vertikalen Symmetrieebene durch die Blockade verlief und durch eine Glasscheibe abgeschlossen war. Die Brennstäbe wurden durch Glasstäbe simuliert. Die Strömungsgeschwindigkeit wurde im Bereich von 1,2 bis 4,5 m/s verändert. Argon wurde entweder in das Totwassergebiet hinter der Blockade oder stromabwärts vor der Blockade eingespeist. Die Menge wurde hierbei von 1 bis 230 Ncm<sup>3</sup>/s variiert (Normaldruck, Normaltemperatur).

Als Ergebnis der durchgeführten Versuche ist folgendes evident:

Das injizierte Gas wird im Totwasser hinter der Blockade kumuliert, und es bildet sich eine Gasblase. Das Strömungsbild des Zweiphasen-Gemisches im Totwasser kann in drei Typen klassifiziert werden, abhängig von der Wassergeschwindigkeit im ungestörten Bereich. Im unteren Geschwindigkeitsbereich kann sich eine stationäre Gasblase nicht aufrecht erhalten, infolge von Auftriebskräften verläßt sie das Totwassergebiet. Im höheren Geschwindigkeitsbereich wird die Gasblase zerteilt durch Strömungskräfte, nur kleine Bläschen zirkulieren im Totwasser. Im mittleren Geschwindigkeitsbereich bleibt eine stationäre Blase erhalten. Die Blasengröße hängt ab von der injizierten Menge und von der Wassergeschwindigkeit.

Aus den Ergebnissen ergibt sich, daß die Möglichkeit des Auftretens von Brennstabversagen infolge Spaltgasansammlung hinter einer Blockade in einem Brennelement des Schnellen Brüters abhängt von den Betriebsbedingungen, speziell von der Kühlmittelgeschwindigkeit.

## Nomenclature

$A_B$ :	Blockage area
$A_O$ :	Total area for main flow
$C_D$ :	Drag coefficient
F:	Force
$R_{eb}$ :	Bubble Reynolds number
$W_{eb}$ :	Bubble Weber number
P:	Pressure
g:	Acceleration of gravity
r:	Radius
v:	Velocity
u:	Relative velocity
$\sigma$ :	Surface tension
$\rho$ :	Density
$\mu$ :	Viscosity

## Subscript

b:	Bubble
g:	Gas
l:	Liquid

<u>Contents</u>	Page
Abstract	
Zusammenfassung	
Nomenclature	
1. Introduction	1
2. Experimental Apparatus and Method	3
3. Flow Pattern of Two-Phase Mixture	4
3.1 Classification	4
3.2 Formation of Gas Cavity	5
4. Rise of Gas Bubble	6
4.1 Rising Velocity due to Buoyancy	6
4.2 Rising Velocity in the Wake	7
4.3 Critical Velocity of Types 1 and 2	8
5. Breakup of Gas Cavity	10
5.1 Cavity Size	10
5.2 Critical Velocity of Types 2 and 3	11
6. Bubble Size Spectrum	12
7. Residence Time	15
8. Concluding Remarks	16
Acknowledgement	17
References	18

## 1. Introduction

Potential pin-to-pin failure propagation mechanisms due to fission gas release in the subassembly of a Liquid Metal Fast Breeder Reactor (LMFBR) are considered to be the following:

- (1) Mechanical effect: transitory mechanical loads on adjacent fuel pins due to pressure pulses caused by fuel pin rupture.
- (2) Thermal effect:
  - Transitory flow change: flow starvation due to increased two-phase frictional pressure loss, upstream flow stagnation or transient flow reversal.
  - Gas blanketing: gas-jet impingement and downstream gas blanketing.
  - Gas bubble entrapment in wakes of flow obstructions.

Up to now, it is expected that the mechanical effect and the thermal effects of a transitory flow change and of gas blanketing cannot cause fuel failure propagation [1].

However, the thermal effect of gas bubble entrapment in the wake of a flow obstruction such as a subchannel blockage is not evident since the behaviour of gas in wakes is not clear.

The phenomenon of gas bubble entrapment in the wake behind a blockage in LMFBR subassembly geometry was inferred from experiments in the sodium loop (KNS) in Kernforschungszentrum in Karlsruhe [2]. However, the information obtained from the experiment is not necessarily enough to know the behaviour of gas in the wake. Specially in sodium loop experiments, the number and the position of bubble detectors, and hence data obtained, are restricted. To discuss the thermal effect, the behaviour of gas in the wake should be made clear. From the view point of the gas behaviour, information may be obtained by direct observations in a water loop.

There are many blockage types which can be postulated; for instance, porous blockage or spherical blockage, etc.. In the present report, a non-porous planar corner blockage is postulated as in the test section of KNS, without taking account of a mechanism to form the blockage. The flow distribution of liquid in the wake behind the blockage could be drawn as Fig. 1.

The release rate of gas due to the rupture of cladding depends on the rupture size, on the gas pressure and on the friction factor through the fuel pellets. The gas pressure, and hence the amount of fission gas in a fuel pin, depends on the power history of the fuel. The friction factor depends on the axial position of rupture and also on the power history. Thus the release rates which were predicted are scattered, depending on rupture conditions; for instance, 0.016 g/s which corresponds to 3 Ncm<sup>3</sup>/s (standard temperature and pressure) for a friction flow of Xenon, for an effective diametral gap of 0.013 mm in fuel region, for an initial gas plenum pressure of 69 bar [3], or 25 g/s (4000 Ncm<sup>3</sup>/s) for isothermal expansion of Xenon with sonic flow, for a circular breach diameter of 1.3 mm, for an initial gas plenum pressure of 69 bar [4]. Therefore, the gas injection rate is required to be changed in the experiment. The liquid velocity is also required to be changed in the experiment since the coolant velocity of the reactor is controlled corresponding to the operating power.

It is the purpose of this report to describe the behaviour of gas in the wake behind the blockage and its dependence on the gas injection rate and the liquid velocity.

Observations were made of the flow patterns of the two-phase mixture, of the bubble size and of the residence time of bubbles in the wake. These items are those that most directly affect the cooling in the wake behind the blockage when fission gas is released in the subassembly.

## 2. Experimental Apparatus and Method

The cross section of the test section used in the present experiment is shown in Fig. 2. The test section represented one half of the fuel subassembly of SNR 300 prototype reactor, divided along the vertical plane of symmetry through the blockage. A glass wall occupied the position of this plane. Thin glass rods (6.1 mm diameter, 7.9 mm pitch) were arranged to simulate fuel pins. A thin plate blockage was installed on the spacer grid in the corner of the test section. The ratio of the blocked area to the total flow area is 0.21.

A schematic side view of the test section is shown in Fig. 3. Water was pumped upwards through the test section and the flow rate measured before the inlet. The mean velocity of the main flow in the test section ranged from 1.2 to 4.5 m/s in the present experiment.

Argon was injected into the test section to simulate fission gases. A schematic diagram of the gas injection system is also shown in Fig. 3. Two holes through the test section wall were provided for gas injection; one of 0.5 mm diameter 50 mm above the blockage for injection into the wake, and one of 0,8 mm diameter 165 mm below the blockage for injection upstream of the wake. In the present report, the case where gas was injected into the wake is called "downstream gas injection", whereas the case where gas was injected into the flow upstream of the blockage is called "upstream gas injection".

In a number of experiments, a gas plenum of volume  $17 \text{ cm}^3$ , simulating the fuel pin volume, was used for a pulsewise gas injection. The gas was supplied from a gas bottle and the initial gas pressure in the plenum was measured at room temperature. Valves permitted the selection of downstream or upstream gas injection. The gas flow rate could be controlled by valves and was measured in steady state conditions by a Rotameter-type flow meter. In the present experiment, the flow rate ranged from 1 to  $20 \text{ Ncm}^3/\text{s}$  (standard temperature and pressure) for the downstream gas injection case and from 10 to  $230 \text{ Ncm}^3/\text{s}$  for the upstream gas injection case.

The behaviour of gas in the wake behind the blockage was directly observed and recorded on cine film. The film speed was varied between 50 and 1000 pictures/second, depending on the conditions of experiments.

### 3. Flow Pattern of Two-Phase Mixture

#### 3.1 Classification

The flow of the two-phase mixture in the wake behind the blockage was observed in both upstream and downstream gas injection cases for a range of gas injection rates and main flow velocities. The gas was continuously injected and the injection rate was kept constant. The following gas behaviour was observed in the wake.

- gas bubbles rising up through the wake.
- gas bubbles standing still in the wake.
- gas bubbles circulating in the wake.

In the present report, a stationary gas bubble with a radius larger than the hydraulic radius of the sub-channel (2.7 mm) is called a "gas cavity" to distinguish it from the other rising or circulating bubbles. Within the range of conditions in the present experiment, the flow patterns which are characterized by these bubbles can be classified into the following three types.

Type 1: Bubbles rise up through the wake without forming a gas cavity.

Type 2: Bubbles circulate around a gas cavity.

Type 3: Bubbles circulate in the wake with no gas cavity formation.

Schematic diagrams of these flow pattern types are shown in Fig. 4. In Type 1 of the upstream gas injection case, gas bubbles coming from upstream of the blockage circulate and join each other in the central region of the wake, forming a larger bubble which then rises up through the wake with no cavity formation. In Type 1 of the downstream gas injection case, gas is directly injected into the wake, forming a larger bubble which then rises up through the wake with no cavity and no circulating bubble. The flow pattern of Type 1 is characterized by rising bubbles. The flow pattern of Type 2 is characterized by the existence of a gas cavity, being further divided into (a) and (b). In Type 2(a), gas bubbles circulate around the gas cavity whose size changes periodically depending on the experimental conditions, the period varying between 1 ~ 10 seconds. Within a single period, the size of the cavity increases gradually and then decreases due to the discharge of the gas from the top of the cavity. In Type

2(b), gas bubbles circulate around the cavity whose size remains almost constant. The typical examples of Types 2(a) and (b) are shown in Fig. 5. In Type 3, small gas bubbles circulate in the wake with no gas cavity formation.

The relation between these types in the downstream gas injection case and in the upstream gas injection case are respectively shown in Figs. 6 and 7 with reference to the gas injection rate and the main flow velocity. As shown in these figures, the pattern is changed from Type 1 to Type 3 in turn with increasing velocity for any rate of gas injection.

As for the critical conditions between the flow pattern types, the following can be said from Figs. 6 and 7.

- The critical velocity of Types 1 and 2 is about 1.9 m/s, independent of the gas injection rate and of the position of gas injection.
- The critical velocity of Types 2 and 3 increases with increasing rate of gas injection.
- The critical velocity of Types 2 and 3 in the downstream gas injection case is higher than in the upstream gas injection case for each rate of gas injection.

### 3.2 Formation of Gas Cavity

The formation of a gas cavity in the wake was observed using high-speed cine film at a film speed of 1000 pictures/second. The behaviour of the gas injected from the gas plenum into the wake (pulsewise injection) is shown in Fig. 8, where the solid line represents the interface of gas and liquid. As shown in this figure the injected gas is accumulated in the wake, forming the gas cavity, and then gas is released from the cavity toward the main flow in the downstream direction. The behaviour of the gas injected from the gas plenum into the flow upstream of the blockage is shown in Fig. 9, where the solid line represents the interface of two-phase mixture (bubbly) and liquid and where the dotted line represents the interface of gas and liquid. Gas bubbles pass through the spacer grid and enter the wake forming a gas cavity. From Figs. 8 and 9 it can be said that the gas is accumulated in the wake, forming a gas cavity.

#### 4. Rise of Gas Bubble

As mentioned in Section 3.1, the flow pattern of Type 1 is characterized by gas bubbles rising through the wake. The buoyant force can be considered to be one of the most important forces which affect the rise of gas bubbles. This section discusses the motion of a gas bubble under the influence of buoyancy.

##### 4.1 Rising Velocity due to Buoyancy

The velocity of a gas bubble rising in a liquid depends on the buoyant force and the drag force. The buoyant force acting on a spherical gas bubble is expressed as follows;

$$F_{buoy.} = \frac{4}{3} \pi r_b^3 (\rho_l - \rho_g) g \quad (1)$$

where  $r_b$  is the bubble radius,  $\rho_l$  and  $\rho_g$  are the densities of liquid and gas, respectively and  $g$  is the acceleration of gravity.

The drag force acting on the bubble is expressed as follows;

$$F_{drag.} = \frac{1}{2} \rho_l u^2 (\pi r_b^2) C_D \quad (2)$$

where  $u$  is the relative velocity of gas and liquid, and  $C_D$  is the drag coefficient. The relative velocity is

$$u = v_g - v_l \quad (3)$$

where  $v_l$  is the liquid velocity and  $v_g$  is the gas bubble velocity which is called "rising velocity".

By neglecting the gas density compared to the liquid density, the steady-state rising velocity of a spherical gas bubble is obtained from Eqs. (1), (2) and (3) as follows;

$$v_g = v_l + \sqrt{\frac{8 r_b g}{3 C_D}} \quad (4)$$

In the special case that  $v_0 = 0$ , the rising velocity is

$$v_g = \sqrt{\frac{8 r_b g}{3 C_D}} \quad (5)$$

The motion of gas bubbles in stagnant liquids has been studied by Peeble and Garber [5] and divided into four types depending on the magnitude of the bubble Reynolds number defined by

$$Re_b = \frac{2 r_b u_g}{\mu} \quad (6)$$

where  $\mu$  is the viscosity.

Two of the four types correspond to the viscous and transition regions and the other two correspond to the turbulent region. In Region 1 of the Reynolds number below 2 corresponding to the viscous region, the motion of a gas bubble can be described by Stokes' law on the assumption that it is spherical. Above  $Re_b = 2$ , the bubble is deformed. The motion in Region 2 corresponding to the transition region is described by modifying the drag coefficient based on Stokes' law. With increasing  $Re_b$ , the bubble deformation becomes large. The two types of motion in Regions 3 and 4 corresponding to the turbulent region result from the variation of gas bubble deformation.

The rising velocity can be calculated by using the drag coefficient equation obtained by Peeble and Garber for each region of the bubble Reynolds number.

#### 4.2 Rising Velocity in the Wake

A diagram of the motion of the gas bubble rising through the wake is shown in Fig. 10. The gas was injected into the flow upstream of the blockage. Gas bubbles coming from the main stream join each other in the central region of the wake, forming a larger bubble, which then rises up through the wake.

In Fig. 10 the shaded regions represent the bubbles before they join together, and the unshaded regions represent the bubble motion after coalescence with the time interval of 1/50 second. The motion is upwards and towards the wall. The rising velocity is obtained from the axial component of the motion. Its value for each axial position in the test section is shown in Fig. 11. As shown in this figure, the rising velocity increases in the axial direction and approaches the main flow velocity. The gas bubble may be accelerated by the main stream.

Between 5 and 7 cm, however, the increasing rate of the rising velocity is small enough to be neglected in comparison with the increasing rate above the position of 7 cm. This shows that the influence of the main stream on the rising velocity is very small in this region. Thus the wake region can be considered to be present below the axial position of 7 cm where the rising velocity is not influenced by the main stream.

In the wake region, the liquid rotates with a velocity distribution. Then it can be considered that the rising velocity in the wake depends on the liquid velocity, specially in the reverse flow region of the wake. However, the rising velocity in the wake, obtained in the experiment, remains almost constant as seen in Fig. 11. The results show that the influence of the liquid velocity on the rising velocity is small even when the bubble rises up nearby the wall. It may be said that the bubble made by coalescence in the central region of the wake rises up, crossing the radial streamlines of the liquid flow, going out from the wake before entering the reverse flow region. Thus the assumption of stagnant liquid may be used for the calculation of the rising velocity in the wake.

The comparison of the rising velocity in the wake between the experimental and the calculational results is shown in Fig. 12, where the solid curve is obtained from Eq. (5) for the rising velocity in stagnant liquid and where the bubble radius is represented with the effective spherical radius obtained by

$$r_b = \frac{1}{2} \sqrt{a \cdot b} \quad (7)$$

where  $a$  is the width and  $b$  is the height of the bubble which can be measured in the photographs. Though the data are scattered, the experimental results are consistent with the calculation, in the limited range of bubble size. Thus it can be said that the gas bubble rises up through the wake due to the buoyant force.

#### 4.3 Critical Velocity of Types 1 and 2

In the lower velocity range, where gas bubbles rise up due to the buoyant force, it may be said that the gas is separated from the liquid in the wake by the rise of the bubble.

From Fig. 12, the effective radius of the rising bubble formed in the central region of the wake is about 6 mm and then the rising velocity corresponding to the radius is 0,15 m/s. When the downward velocity of liquid against the bubble is lower than this velocity, the gas rises up, being separated from the liquid. With the increasing velocity of the main flow, the downward velocity of liquid against the rising bubble increases and finally the bubble moves down with the liquid, resulting in no separation of gas and liquid. The existence of the gas cavity in the wake results from no separation of gas and liquid. Then the rising velocity due to the buoyant force can be related to the critical velocity of Types 1 and 2.

A discussion of the critical velocity is concerned with the liquid velocity in the reverse flow region where the downward velocity is higher than in any other region of the wake. Table 1 shows the reverse flow velocity which was measured from the movement of bubbles (nearby the wall) with a radius of 0,5 mm. The rising velocity of the bubble due to the buoyant force is small enough to be neglected in comparison with the reverse flow velocity shown in this table. Then it is sufficient to consider that Table 1 shows the liquid velocity in the reverse flow region of the wake. As seen in this table, the main flow velocity is about three times higher than the reverse flow velocity in the present experiment (water). If it is assumed that the separation occurs in the reverse flow region, the critical velocity should be about

$$0.15 \times 3 = 0.45 \text{ m/s} \quad (8)$$

However, the experimental results in Figs. 6 and 7 show that the critical velocity is 1.9 m/s. The discrepancy of the critical velocity between the experimental and the calculated values shows that the separation of gas and liquid does not occur in the reverse flow region. The gas is separated from the liquid before entering the reverse flow region and as a result the critical velocity of Types 1 and 2 has the higher value of 1.9 m/s. From the comparison between the rising velocity and the reverse flow velocity, it can be said that the separation of gas and liquid occurs in the region where the downward velocity of liquid is less than a quarter of the maximum reverse flow velocity.

## 5. Breakup of Gas Cavity

### 5.1 Cavity Size

The dependence of the cavity size on the main flow velocity under the various rates of steady gas injection is shown in Fig. 13, where the cavity size is represented with the effective spherical radius obtained by Eq. (7). In the velocity range corresponding to Type 2(a), where the cavity size changes periodically, the cavity size is represented with a mean value and an amplitude of the change of size. As shown in this figure, the cavity size decreases with increasing velocity of the main flow for each rate of gas injection. Under conditions of constant gas injection rate, the cavity has a maximum radius at the critical velocity of Types 1 and 2, whereas the cavity has a minimum radius at the critical velocity of Types 2 and 3.

Figure 14 shows the change of the cavity size after the termination of gas injection, where the gas injection rate applies before termination. At a main flow velocity of 2 m/s, the cavity size showed periodic behaviour up to the termination of gas injection, but not afterwards.

The initial size is represented with a mean value and an amplitude of the change of size. As revealed in this figure, the cavity size decreases gradually with time after the termination of gas injection. The gas cavity may be broken up by liquid flow forces in the wake, resulting in the decrease of the cavity size. On the other hand, the gas is accumulated in the wake as described in Section 3.2. Therefore, it can be considered that the gas cavity is sustained by two contrary effects; formation of the cavity due to gas accumulation and breakup of the cavity by liquid flow forces.

The dependence of the cavity size on the gas injection rate and the main flow velocity, shown in Fig. 13, can be described by the mass balance of gas due to the two contrary effects. With increasing rate of the gas injection, the supply of gas to the cavity may increase. Specially in the downstream gas injection case, the gas is directly injected and accumulated in the wake, as shown in Fig. 8. Then the cavity size is increased by the increased supply of the gas with increasing rate of gas injection under conditions of constant velocity of the main flow. With increasing velocity of the main flow, the liquid flow forces acting on the cavity may be increased, resulting in the decrease of the cavity size under conditions of constant gas injection rate.

In the lower velocity range corresponding to the flow pattern of Type 2(a), where the cavity size is changed periodically, the liquid flow forces acting on the cavity may be small. Thus the discharge of gas from the cavity of Type 2(a), which causes the change of the cavity size, can be considered to result from the excess supply of gas to the cavity.

### 5.2 Critical Velocity of Types 2 and 3

The cavity size decreases with increasing velocity of the main flow, as mentioned in Section 5.1, and finally the cavity disappears in the higher velocity range corresponding to the flow pattern of Type 3. The liquid flow forces acting on the cavity may be increased with increasing velocity of the main flow, resulting in the complete breakup of the cavity in the higher velocity range.

As mentioned in Section 3.1, the critical velocity of Types 2 and 3 increases with increasing rate of gas injection. This can be also described by the mass balance of gas due to the two contrary effects on the cavity. The increase of the gas injection rate causes the supply of gas to the cavity to increase, whereas the increase of the main flow velocity may cause liquid flow forces acting on the cavity to increase. Thus, for complete breakup of a gas cavity the main flow velocity should increase against the increased supply of gas to the cavity.

As mentioned also in Section 3.1, the critical velocity in the upstream gas injection case is lower than in the downstream gas injection case. In the upstream gas injection case, some of the gas injected into the flow upstream of the blockage enters the wake, and the rest is swept past with the main flow. Thus the critical velocity in the upstream gas injection case is lower because the supply of gas to the wake is lower for any injection rate. From the comparison of the cavity size in Fig. 13, it is estimated that about 2 % of the gas injected into the flow upstream of the blockage enters the wake forming a gas cavity.

## 6. Bubble size spectrum

The bubble size was measured from photographs and a bubble size distribution obtained. Though the radius of gas bubbles which can be measured is limited by the photographic resolution, bubble size histograms for resolvable bubbles have been obtained for a range of experimental conditions. Figures 15 and 16 show the dependence of the bubble size spectrum on gas injection rate and on main flow velocity. As shown in these figures, the bubble size spectrum is influenced markedly by the main flow velocity but not significantly by the gas injection rate. With increasing velocity of the main flow, the spectrum becomes sharper and the radius corresponding to the peak of the spectrum is decreased.

The velocity dependence of the bubble radius is shown in Fig. 17 for both the downstream and the upstream gas injection cases, where the bar represents the standard deviation from the mean value obtained from the bubble size spectrum. A difference of bubble radius between these cases is distinguishable only in the lower velocity range corresponding to the flow pattern of Type 1. In the case of upstream gas injection, the gas bubbles pass through a spacer grid before entering the wake, and are probably broken up into smaller bubbles during their passage. The hydraulic radius of the sub-channel at the spacer grid is about 1 mm, which agrees well with the bubble size observed in the upstream gas injection case. On the other hand, in the case of the downstream gas injection, the gas is injected directly into the wake without going through the spacer grid, and the bubble size at low main flow velocities is about 5 times greater. It may be said that in the lower velocity range the bubble radius in the wake is influenced by the position of gas injection. However, no influence of the position of gas injection on the bubble radius can be seen at higher velocities corresponding to the flow patterns of Types 2 and 3.

In discussing the bubble size in the higher velocity range, the bubble Weber number is considered. The bubble Weber number is defined as the ratio of the inertia force to the surface tension, expressed as follows;

$$We_b = \frac{2 r_b \rho u^2}{\sigma} \quad (9)$$

where  $\sigma$  is the surface tension. The velocity distribution in the wake shows large velocity gradient, particularly at the boundary with the main flow. The bubble circulating in the wake may suffer an inertia force due to the relative velocity of gas and liquid caused by the velocity gradient. The radial gradient of the liquid velocity would be more steep than the tangential gradient in the wake. The relative velocity of gas and liquid caused by the radial gradient of the liquid velocity is expressed as follows;

$$u = r_b \left. \frac{\partial v_l}{\partial r} \right|_{cb} \quad (10)$$

where  $\left. \frac{\partial v_l}{\partial r} \right|_{cb}$  represents the radial gradient of liquid velocity, defined at the center of bubble moving with the liquid. Then the Weber number is expressed as follows;

$$We_b = r_b^3 \frac{2\rho_l}{\sigma} \left( \left. \frac{\partial v_l}{\partial r} \right|_{cb} \right)^2 \quad (11)$$

The radial gradient of the liquid flow on the main stream side of the wake may be more steep than the gradient on the wall side. Then the following assumption is made for the radial gradient;

$$\begin{aligned} \left. \frac{\partial v_l}{\partial r} \right|_{cb} &\approx \frac{\Delta v_l}{\Delta r} \\ &\equiv \frac{v_m}{r_w} \end{aligned} \quad (12)$$

where  $v_m$  is the liquid velocity on the main stream side of the wake and  $r_w$  is the effective spherical radius of the wake. The liquid velocity on the main stream side is expressed as follows;

$$\begin{aligned} v_m &= \frac{1}{2} (v_0 + v_t) \\ &= v_0 \cdot \frac{1 - \frac{A_B}{2A_0}}{1 - \frac{A_B}{A_0}} \end{aligned} \quad (13)$$

where  $v_0$  is the main flow velocity,  $v_t$  is the liquid velocity at the edge of the blockage,  $A_B$  is the blocked flow area and  $A_0$  is the total area for the main flow. The effective radius of the wake is expressed as follows;

$$r_w = \frac{1}{2} \sqrt{\frac{6(A_B + A_f)}{\pi}} \quad (14)$$

where  $A_f$  is the cross sectional area of glass rods within the blockage and the factor 6 is based on the blockage geometry. Under the present experiment,  $v_m$  and  $r_w$  are respectively

$$\left\{ \begin{array}{l} v_m = 1.1 v_0 \quad (m/s) \\ r_w = 2.1 \times 10^{-2} \quad (m) \end{array} \right. \quad (15)$$

Accordingly, the bubble Weber number is then expressed as follows;

$$We_b = (5.5 \times 10^3) r_b^3 v_0^2 \frac{\rho_l}{\sigma} \quad (16)$$

From the expression of the Weber number, the following equation is obtained for the bubble radius.

$$r_b = (5.7 \times 10^{-2}) v_0^{-\frac{2}{3}} \left( We_b \frac{\sigma}{\rho_l} \right)^{\frac{1}{3}} \quad (17)$$

The calculational results obtained by Eq. (17) for various Weber number are shown in Fig. 17 with solid curve. As seen in this figure, the Weber number of the bubbles in the wake ranges between 0.1 and 10. Specially in the higher velocity range corresponding to the flow patterns of Types 2 and 3, the experimental results of the bubble radius are described by the solid curve with  $We_b = 1$ . It is mentioned that the calculation is based on the assumption of (12) for the liquid velocity gradient. Though the liquid flow is disturbed on the main stream side, the radial gradient of the time-smoothed velocity is considered to be approximately represented by the ratio of  $v_m$  to  $r_w$ . Then it can be said that the bubbles are broken up into smaller bubbles of  $We_b \approx 1$  by the inertia force of the liquid flow on the main stream side of the wake. Only bubbles with a Weber number of about unity can be present in the wake.

A gas cavity has a Weber number larger than unity since the cavity size is larger than the bubble size. Thus the cavity is broken up by the inertia force of the liquid flow on the main stream side of the wake, but is constantly renewed by the further accumulation of gas in the wake.

## 7. Residence Time

As shown in Fig. 14, the cavity size is gradually decreased with time after the termination of gas injection, and finally the cavity disappears. The residence time is defined as the time from the termination of gas injection to the disappearance of the cavity. The dependence of the residence time on the main flow velocity is shown in Fig. 18, where the gas injection rate applies before termination and affects the initial size of the cavity. As shown in this figure, the residence time depends on the main flow velocity, decreasing with the increasing velocity of the main flow.

The residence time of gas bubbles is also defined as the time from the termination of gas injection to the disappearance of the bubbles. The dependence of the residence time on the main flow velocity is shown in Fig. 19, where the gas injection rate applies before termination. In the lower velocity range corresponding to the pattern of Type 1, the gas is separated from the liquid in the wake by the rise of a larger bubble made by coalescence of small bubbles as mentioned in Section 3. In the higher velocity range corresponding to the pattern of Type 3, small gas bubbles circulate in the wake and gradually disappear from the wake. In the velocity range in between, corresponding to the pattern of Type 2, small bubbles circulate around a gas cavity whose size is gradually decreased with time after the termination of gas injection and finally bubbles disappear after the complete breakup of the cavity. As shown in Fig. 19 the residence time of gas bubbles depends on the main flow velocity as does the residence time of gas cavity.

## 8. Concluding Remarks

Gas may, under some conditions, accumulate in the wake behind a blockage, forming a stable gas cavity.

The two-phase flow patterns in the wake are classified into three types depending on the velocity range of the main flow. In the lower velocity range corresponding to the flow pattern of Type 1, a gas cavity cannot remain in the wake, but rises up as a single bubble due to the buoyant force. In the higher velocity range corresponding to the flow pattern of Type 3, the gas cavity is broken up by the inertia force of the liquid flow on the main stream side of the wake, only small gas bubbles circulating in the wake. In the velocity range in between, corresponding to the flow pattern of Type 2, a gas cavity is present in the wake, engulfing the glass rods simulating fuel pins. The velocity range corresponding to the flow pattern of Type 2 is within the operating range of the coolant velocity of typical LMFBRs. Though the physical properties of sodium are different from those of water, the formation of a gas cavity in the wake behind a blockage in a LMFBR subassembly can be considered possible.

The size of the cavity depends on the gas injection rate and on the main flow velocity, decreasing with decreasing rate of gas injection and with increasing velocity of the main flow. The residence time of the cavity also depends on the main flow velocity, decreasing with increasing velocity of the main flow. The results obtained in the present experiment show that the main flow, and hence the liquid flow in the wake, affects the flow pattern, the cavity size, the bubble size, and the residence time of the cavity and of the bubbles. Furthermore, it is mentioned that the flow pattern was changed from Type 1 to Type 3 in turn with increasing velocity for any rate of gas injection in the range of present experimental conditions. Therefore, the initiation of fuel pin dryout caused by the release of fission gas at a blockage in a LMFBR can be considered to depend on the operating conditions of the reactor, specially on the coolant velocity.

Acknowledgement

The author is deeply indebted to Dr. W. Pepler for his valuable discussions and kind encouragement in performing this study.

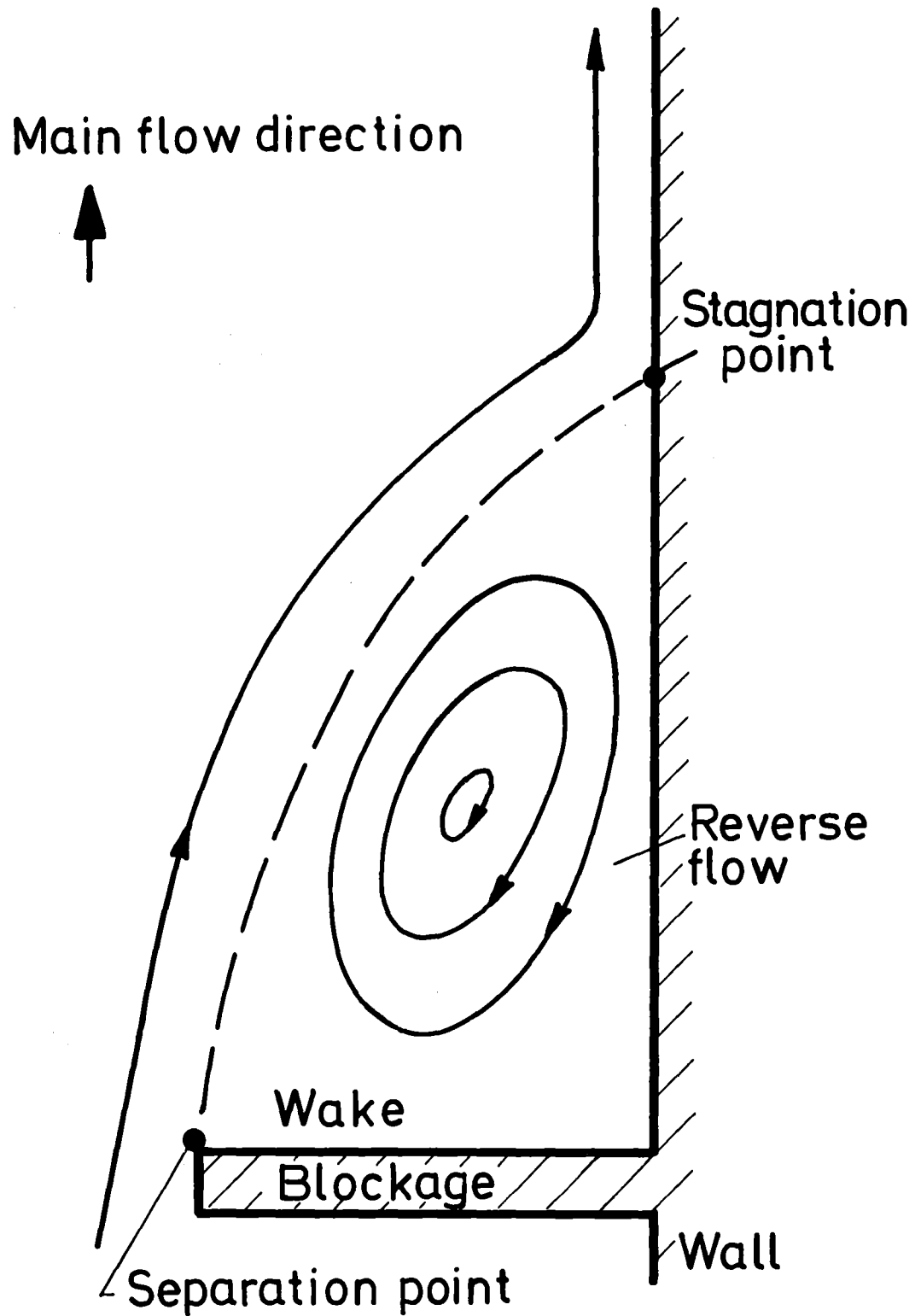
The author wishes to express his thanks to the colleagues of the Institut für Reaktorentwicklung, Kernforschungszentrum Karlsruhe, for their technical assistance in carrying out these experiments.

References

- [1] R.M. Crawford, W.W. Marr, A. Padilla, Jr., and P.Y. Wang  
"The Safety Consequences of Local Initiating Events in an LMFBR"  
ANL-75-73. (Dec. 1975)
- [2] A.J. Clare, F. Huber, W. Till and W. Pepler  
"Preliminary Results of the Temperature Distribution and Boiling  
Behaviour behind a Wall Blockage in a 169 Pin Bundle"  
8. Liquid Metal Boiling Working Group Meeting, October 9, 1978, Mol
- [3] R.E. Murata, K.E. Gregoire and C.N. Craig  
"Friction Factors and Model for Gas Release from Failed LMFBR Fuel  
Rods"; GEAP-13989 (Sept. 1973)
- [4] J.B. Van Erp, T.C. Chawla and R.E. Wilson  
"Potential Fuel Failure Propagation Due to Fission-Gas Release  
in LMFBR Subassemblies"  
ASME, 72-WA/NE-14 (Nov. 1972)
- [5] F.N. Peebles and H.J. Garber  
"Studies on the Motion of Gas Bubbles in Liquids"  
Chemical Engineering Progress, Vol. 49, No. 2, pp. 88-97  
(Feb. 1953)

Main flow velocity $v_o$ [ m/s ]	Reverse flow velocity, $v_{rev}$ [ m/s ]				$\frac{v_o}{v_{rev}}$
	Under steady injection (Downstream: 11.5 Ncm <sup>3</sup> /s)	After the termination of injection			
		t=1s	t=3s	t=5s	
2.0	0.7	-	-	-	2.9
3.0	1.1	1.1	1.1	1.1	2.7
4.5	1.8	-	-	-	2.5

Table 1: Liquid Velocity in the Reverse Flow Region of the Wake



KJK

**Fig. 1 Schematic Diagram of Flow Distribution in the Wake Behind a Corner Blockage**

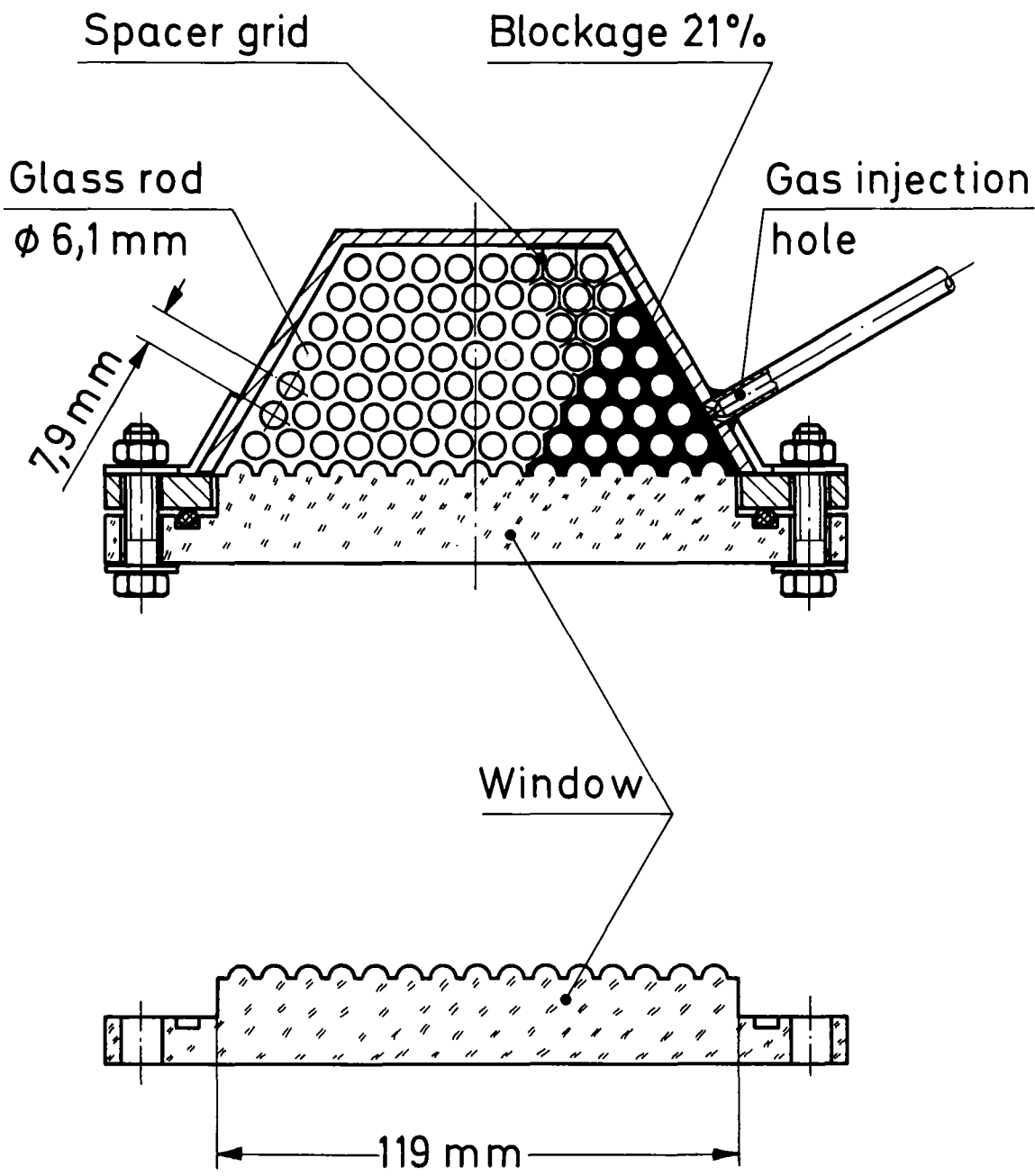
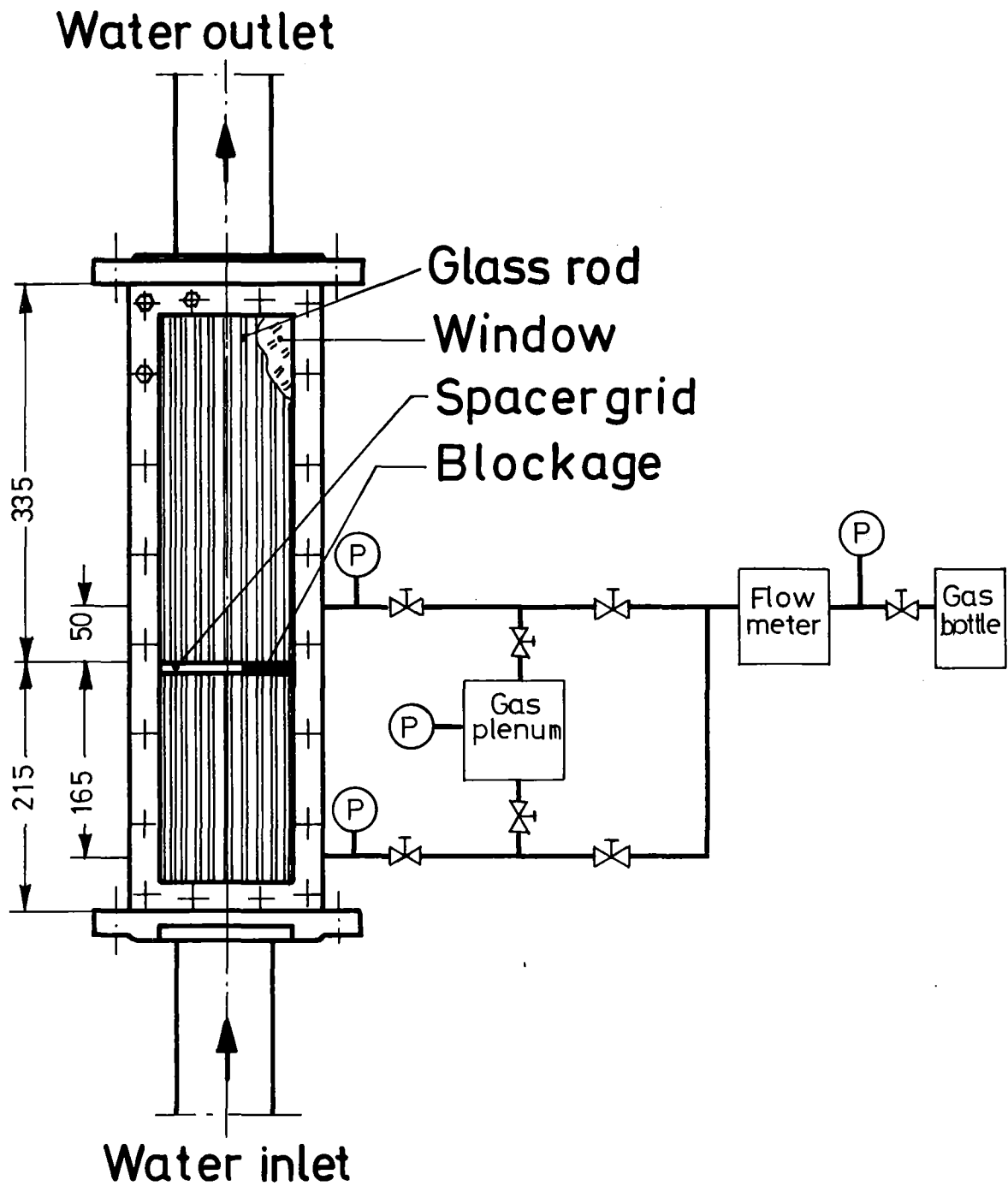
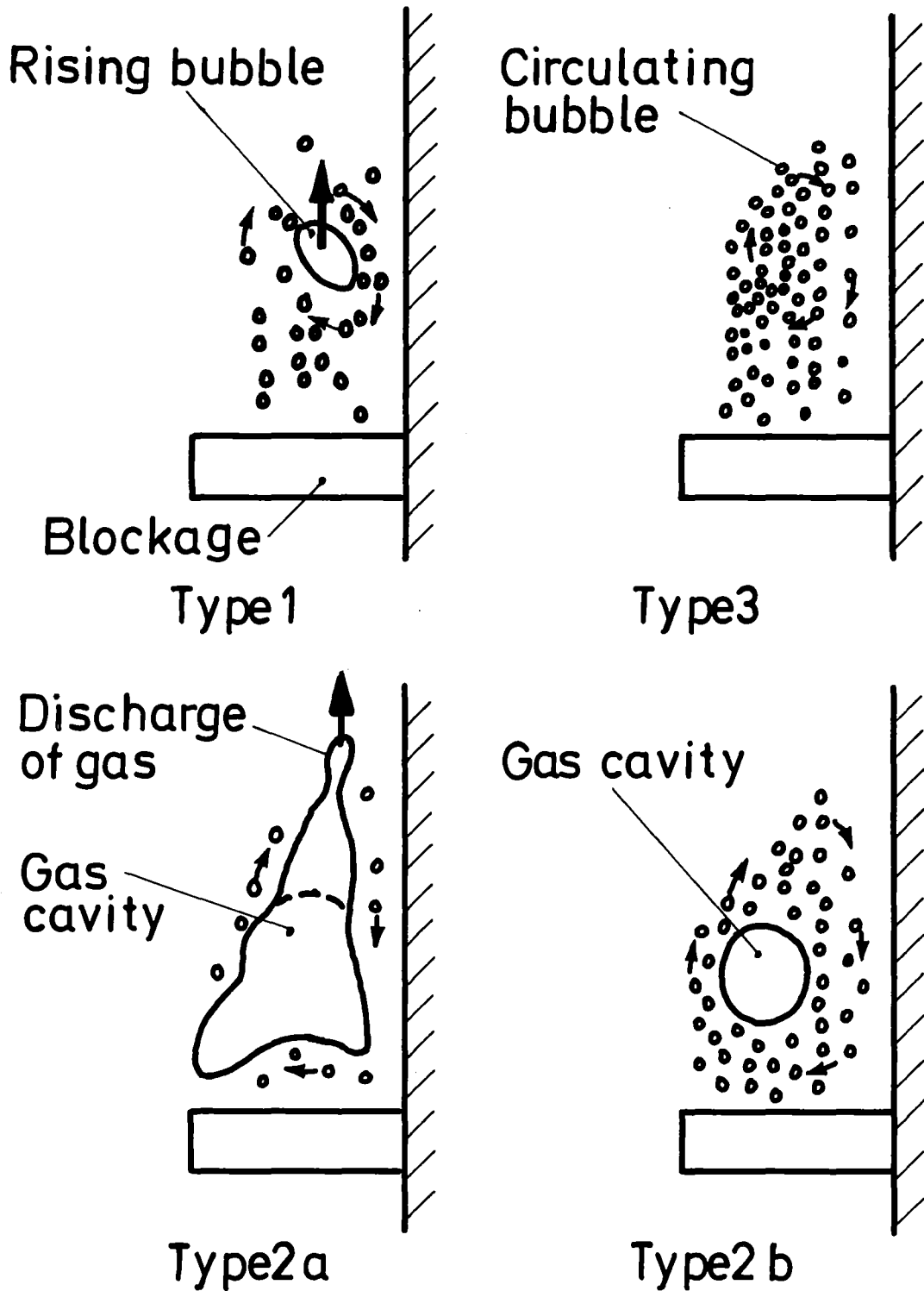


Fig. 2 Cross Section of Test Section

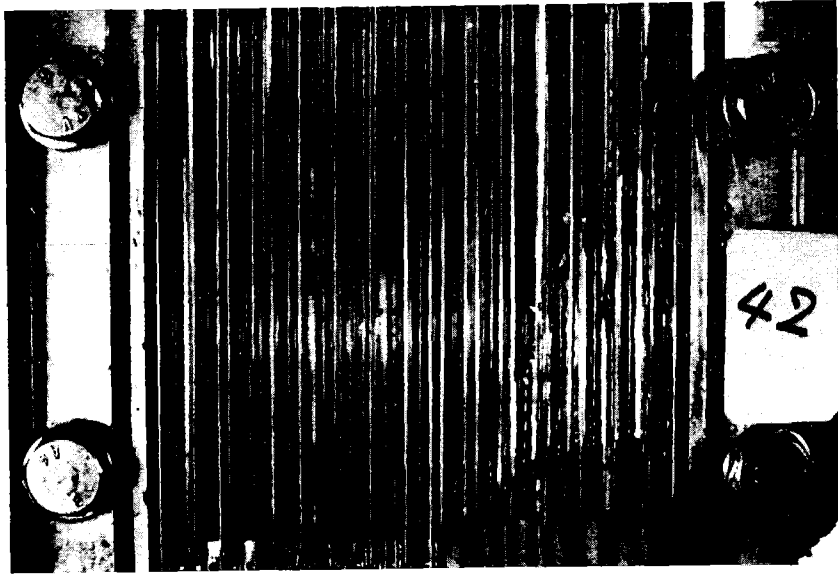


**Fig. 3 Schematic Side View of Test Section and Installed Gas Injection System**

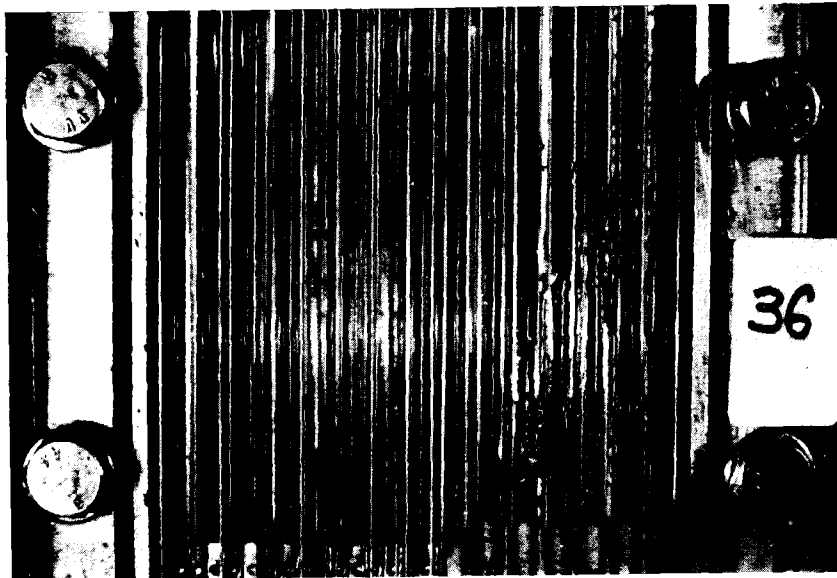


KJK

Fig. 4 Schematic Diagrams of Two-Phase Flow Patterns in the Wake



Type2 a  
2.1 m/s, 11.5 Ncm<sup>3</sup>/s

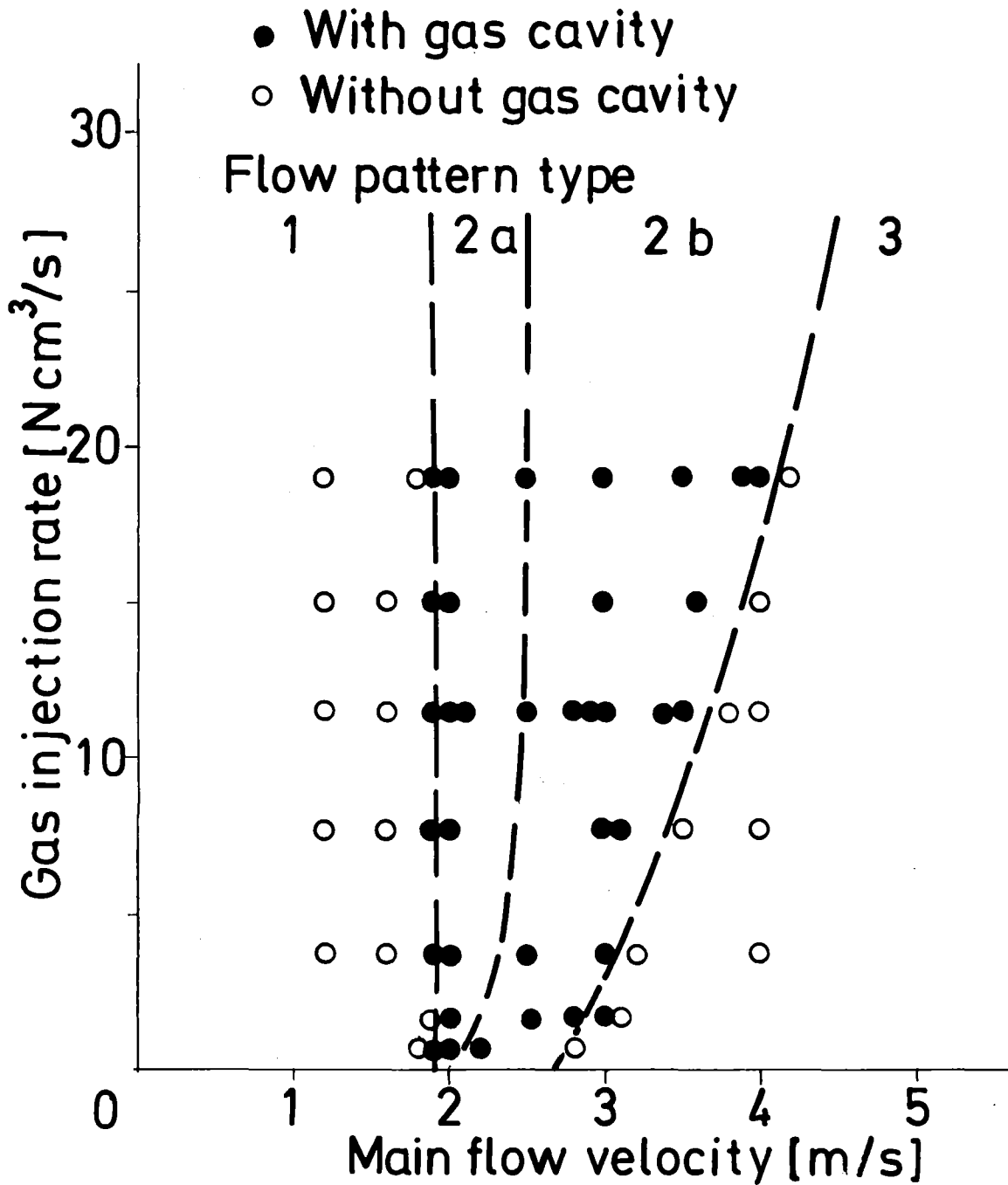


Type2 b  
2.8 m/s 11.5 Ncm<sup>3</sup>/s

---

KIK

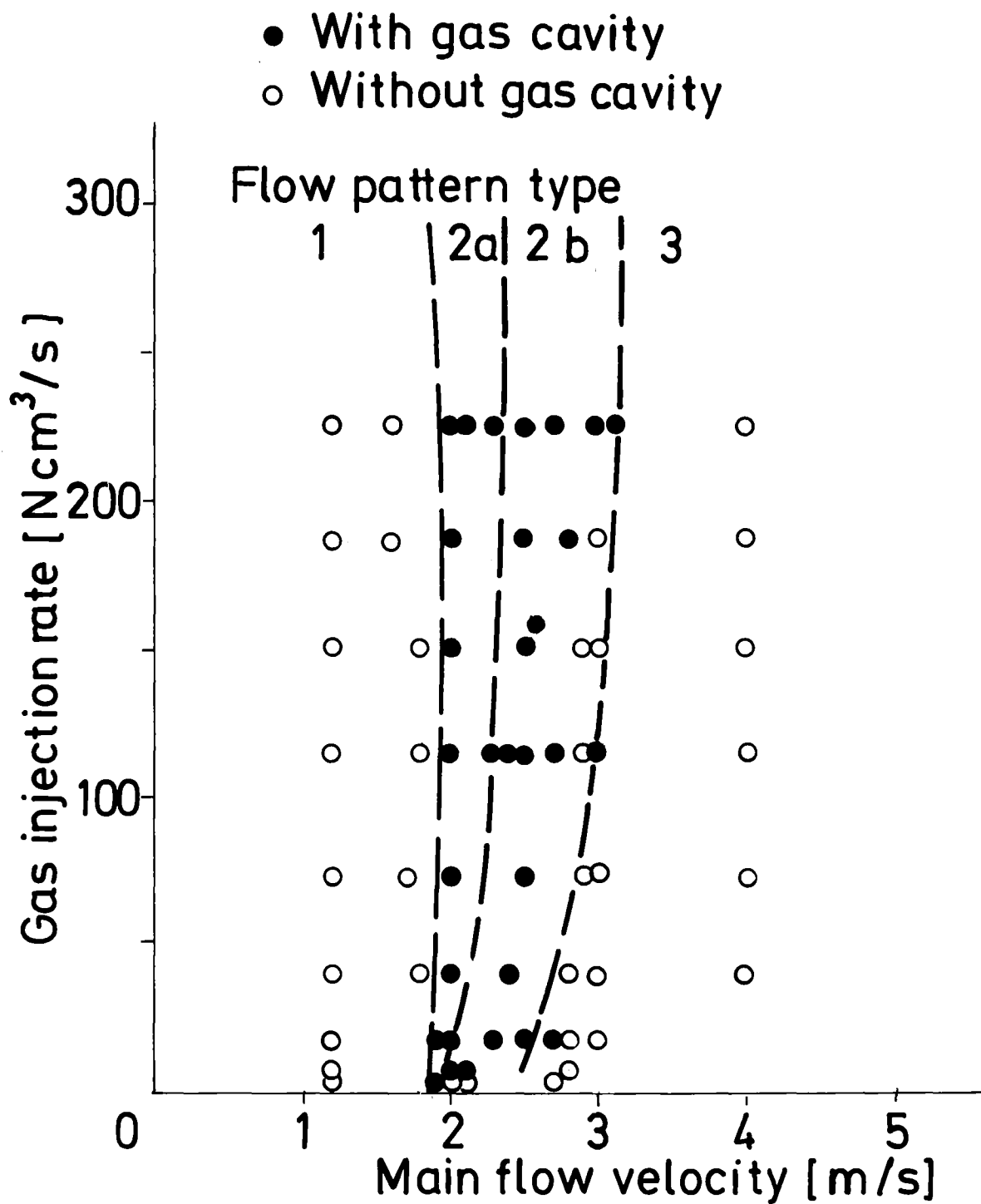
Fig. 5 Downstream Gas Injection



Down stream gas injection



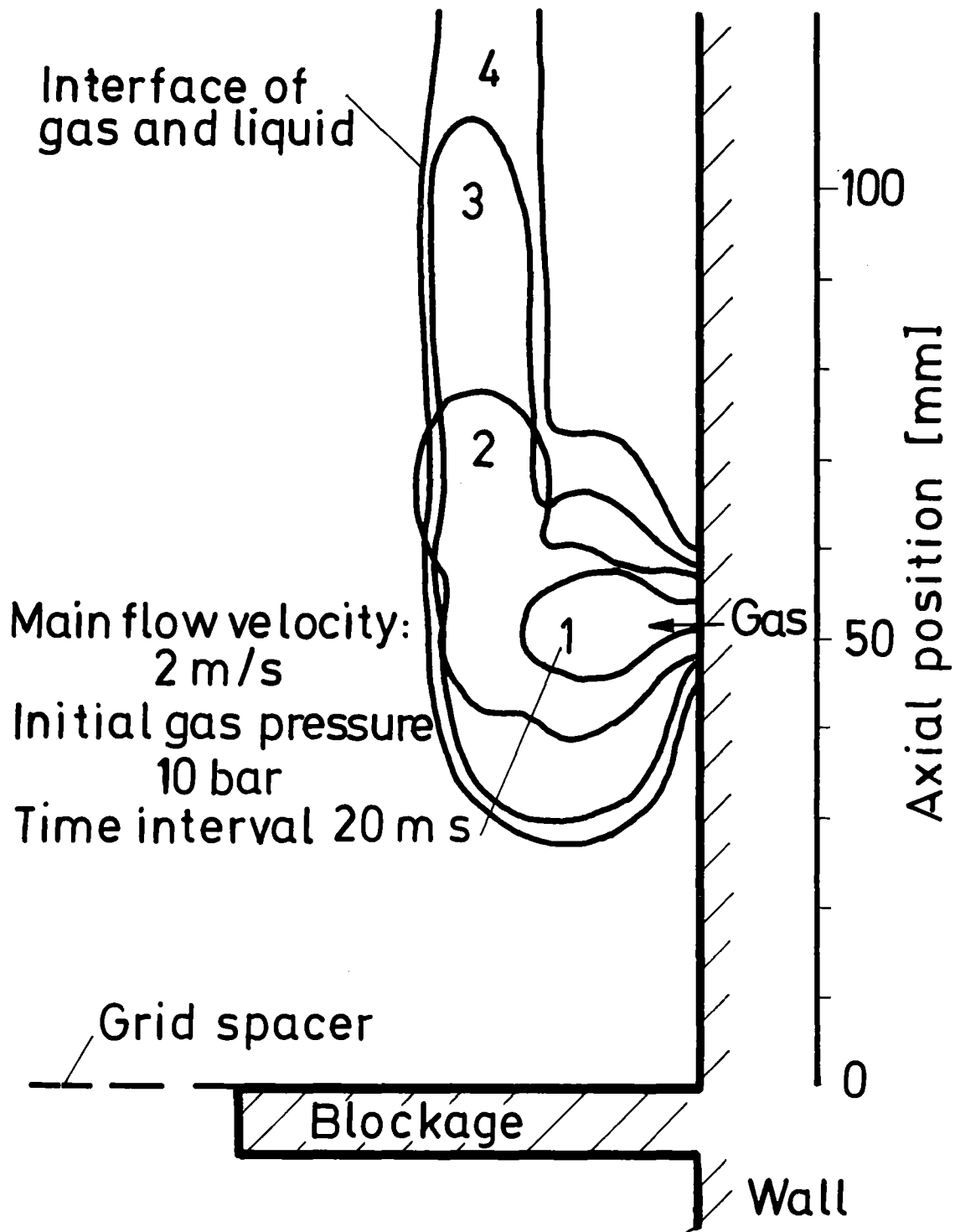
Fig. 6 Relation Between Flow Pattern, Gas Injection Rate and Main Flow Velocity



Upstream gas injection



Fig. 7 Relation Between Flow Pattern, Gas Injection Rate and Main Flow Velocity



KIK

**Fig. 8 Gas Behaviour in the Wake just after Start of Downstream Gas Injection**

Main flow velocity: 2 m/s  
Initial gas pressure: 30 bar  
Time interval: 200 ms

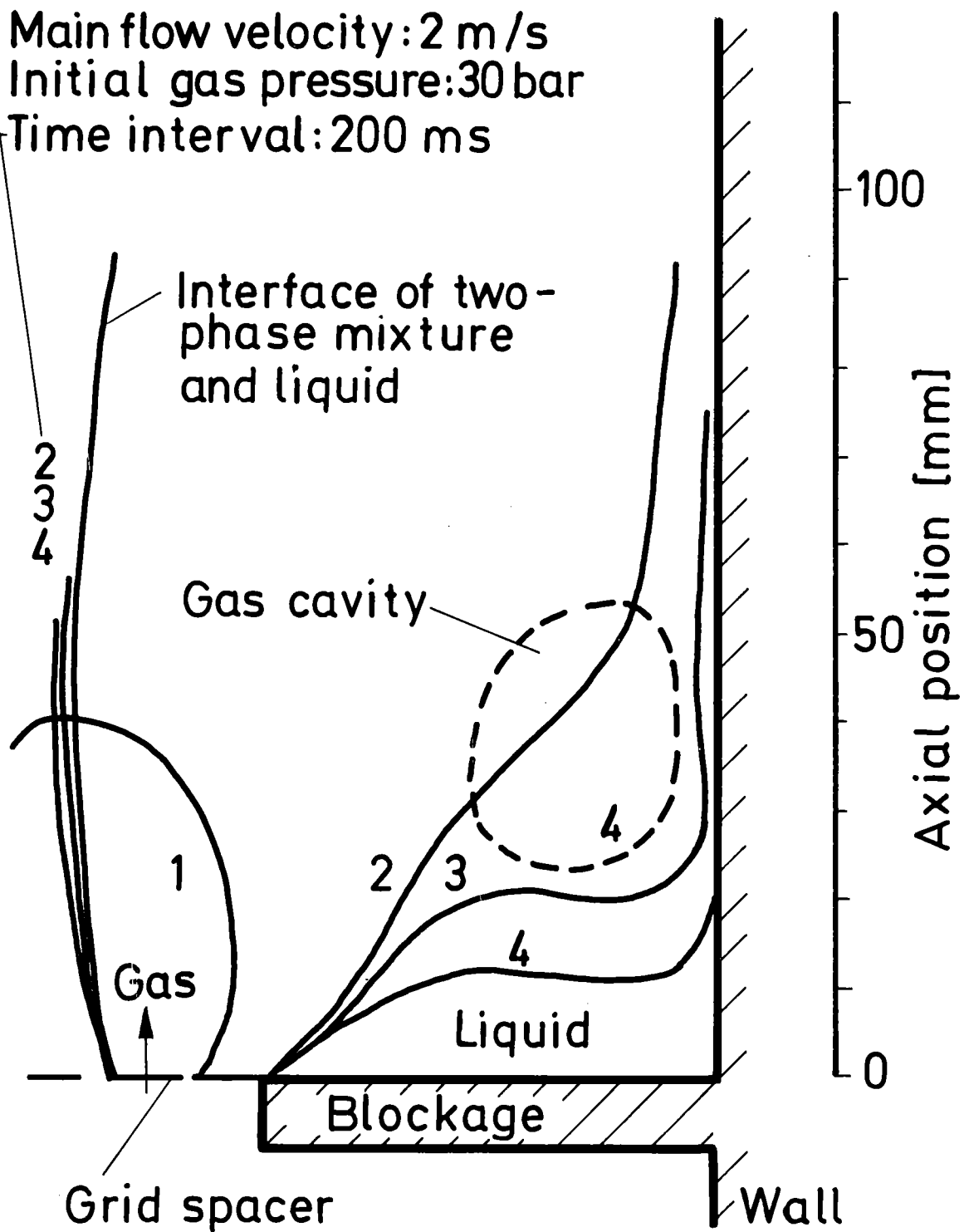
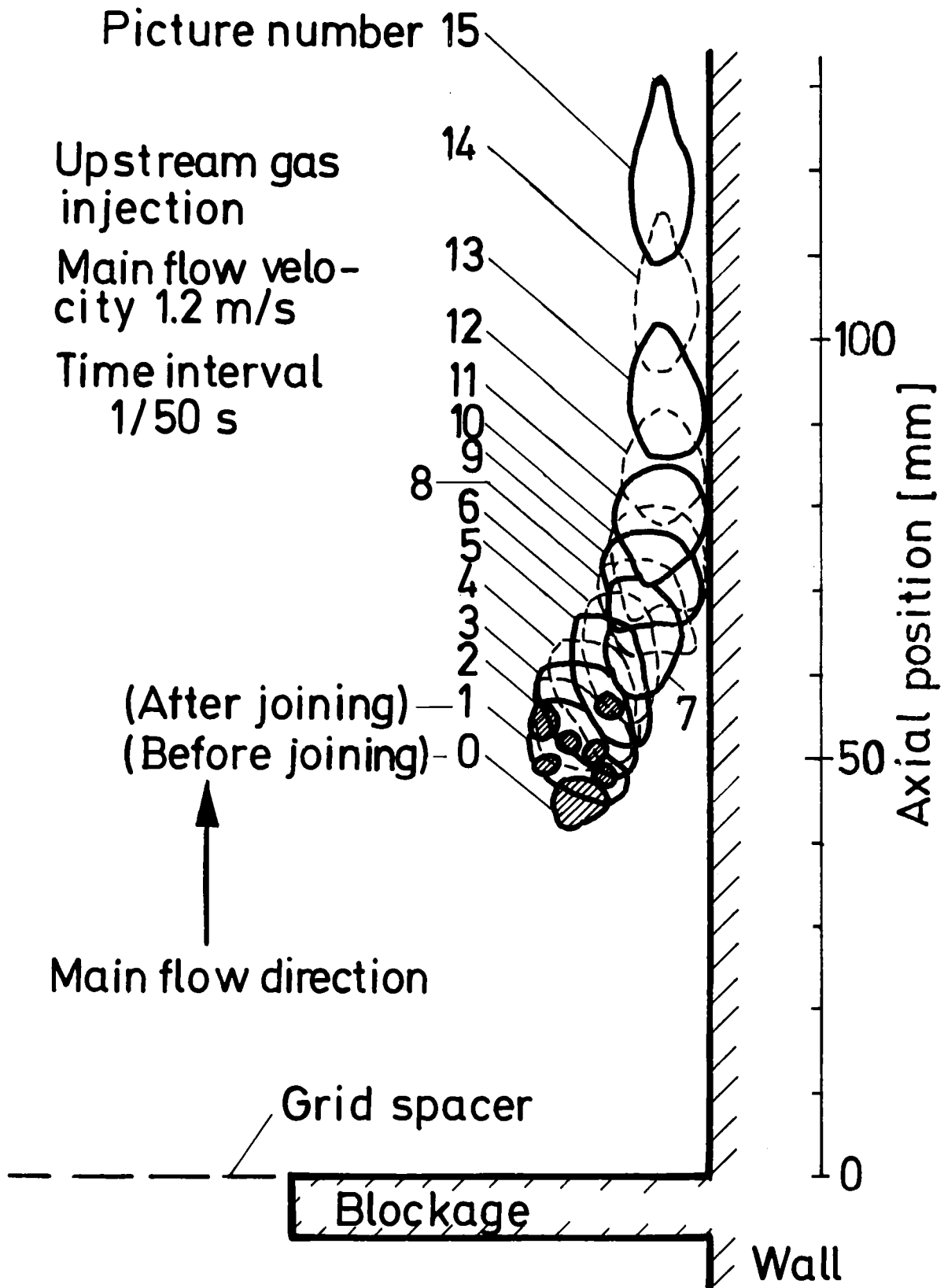
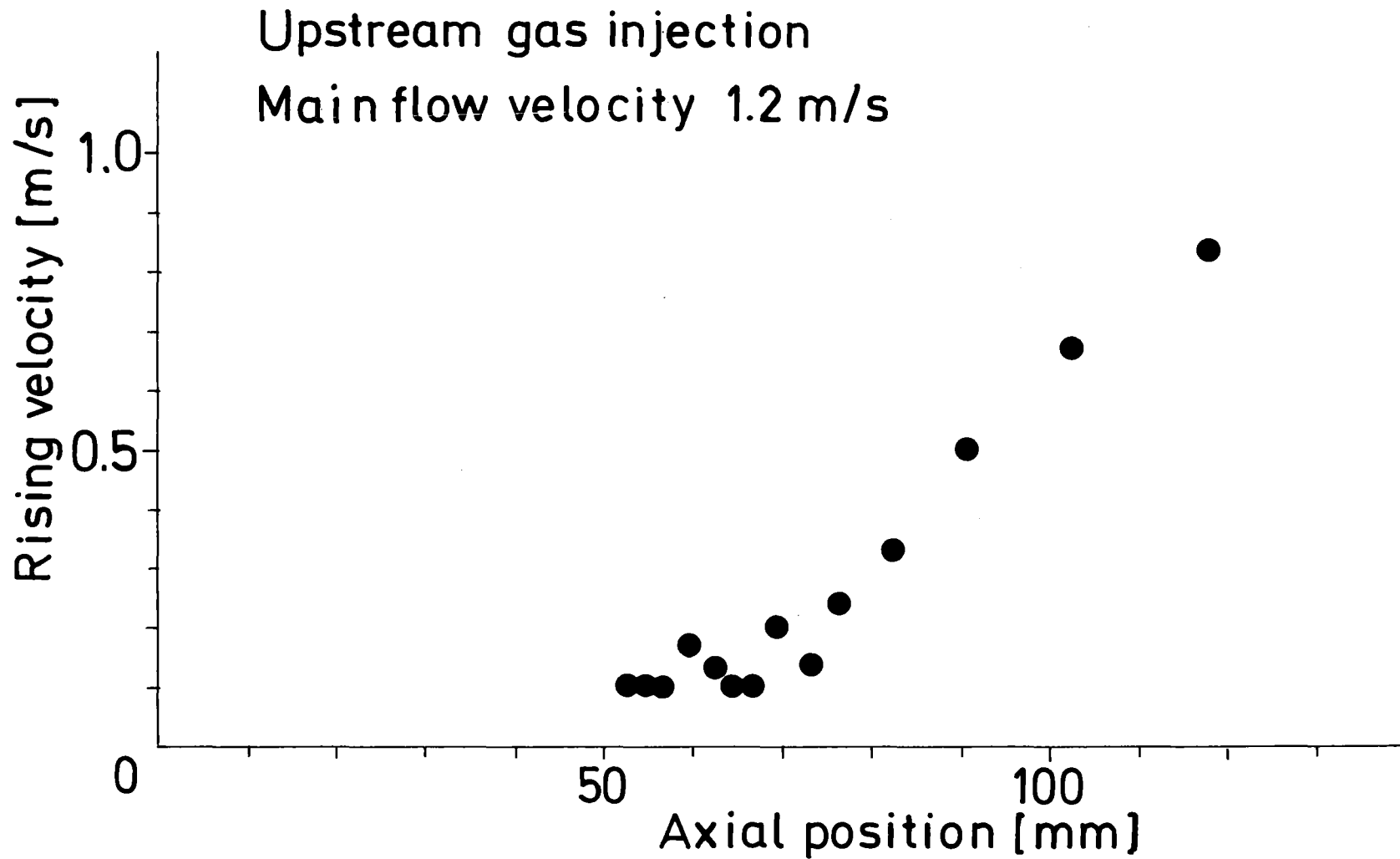


Fig. 9 Gas Behaviour in the Wake just after Start of Upstream Gas Injection



**Fig.10 Diagram of Gas Bubble Behaviour in the Wake under Lower Velocity of Liquid**



KJK

Fig.11 Rising Velocity Versus Axial Position

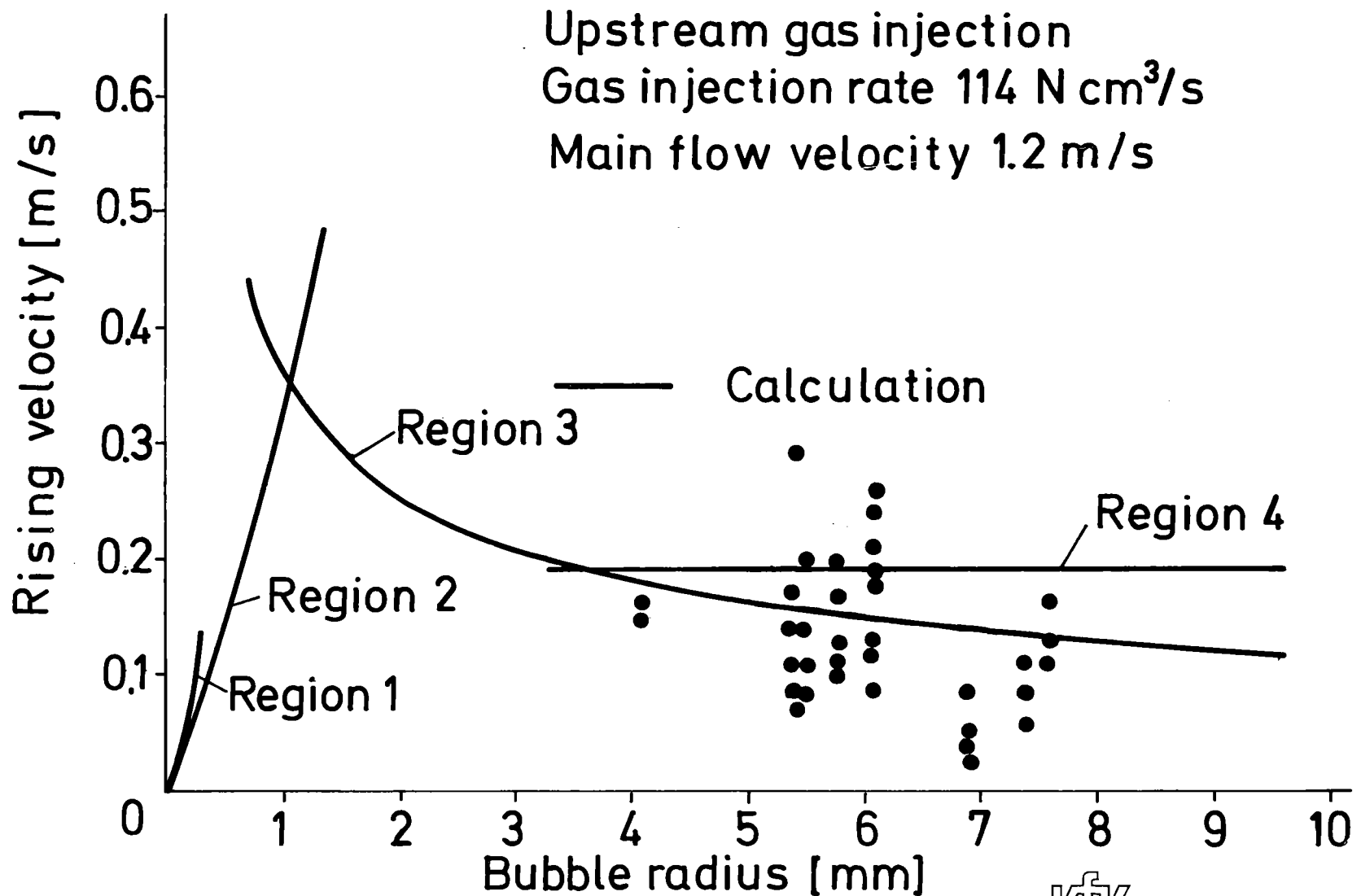


Fig.12 Comparison Between Experimental and Calculational Results of Rising Velocity

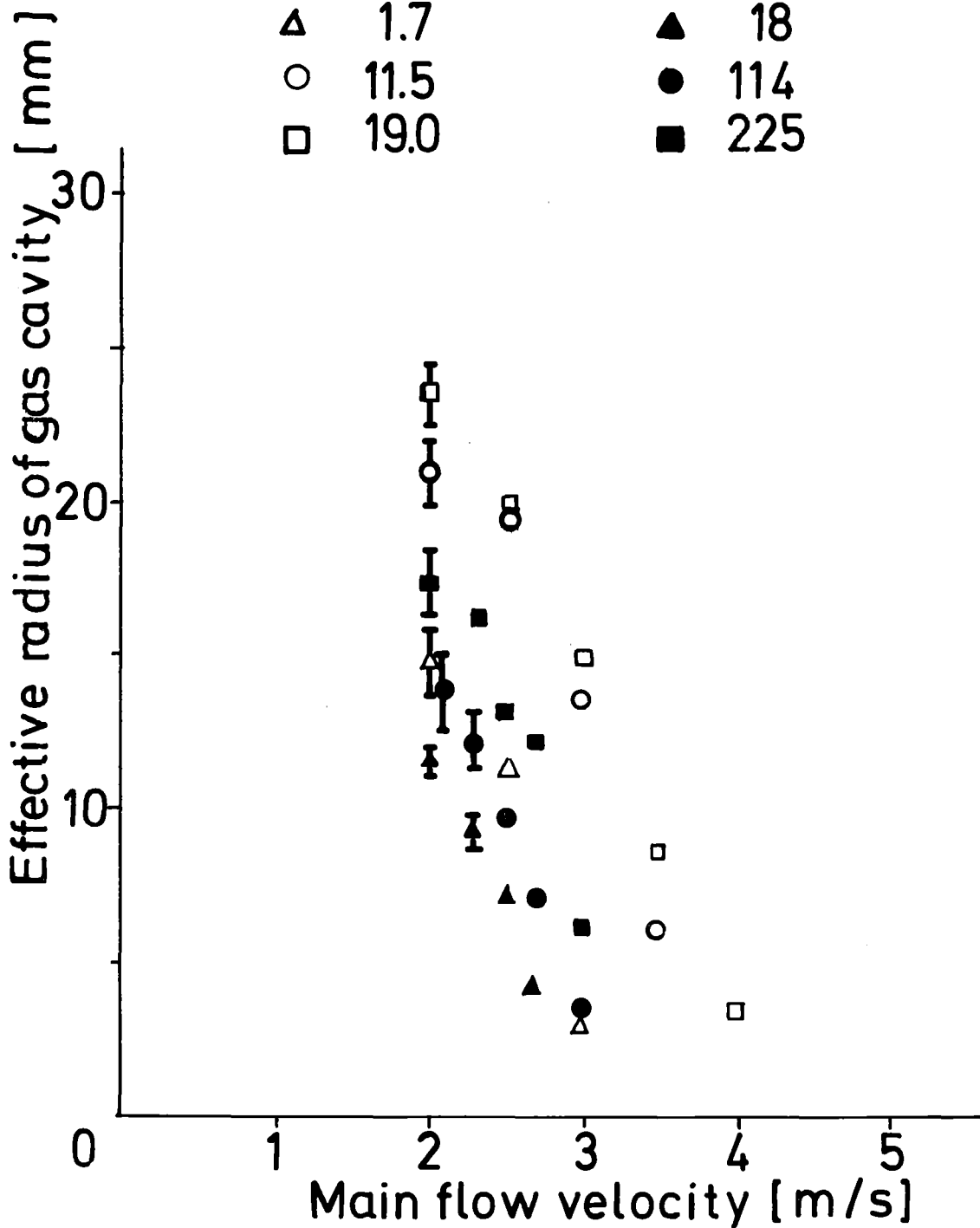
Gas injection rate  $\text{Ncm}^3/\text{s}$

Downstream

Upstream

$\triangle$  1.7  
 $\circ$  11.5  
 $\square$  19.0

$\blacktriangle$  18  
 $\bullet$  114  
 $\blacksquare$  225



KJK

Fig.13 Dependence of Cavity Size on the Liquid Velocity for Various Gas Injection Rates

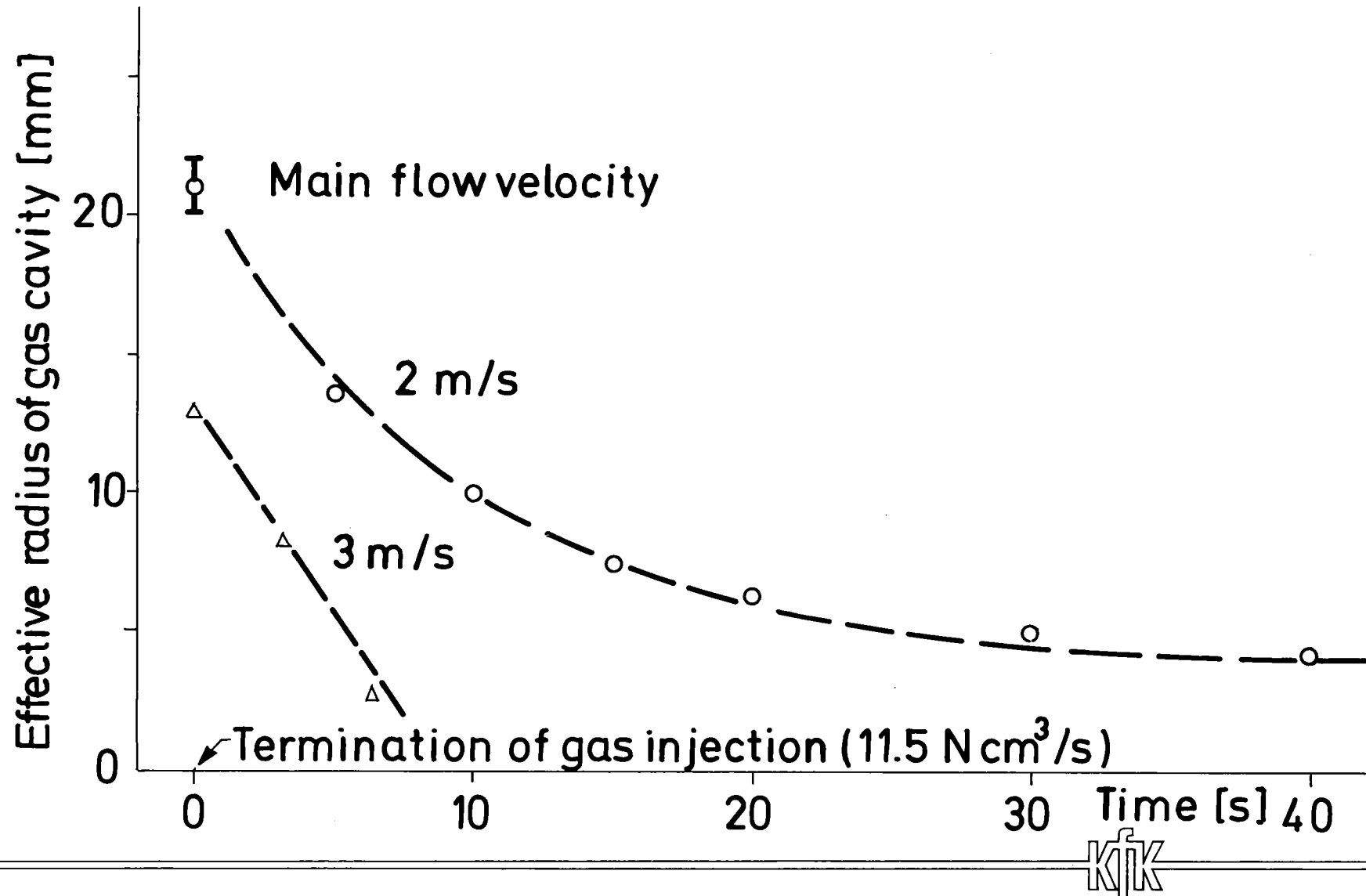
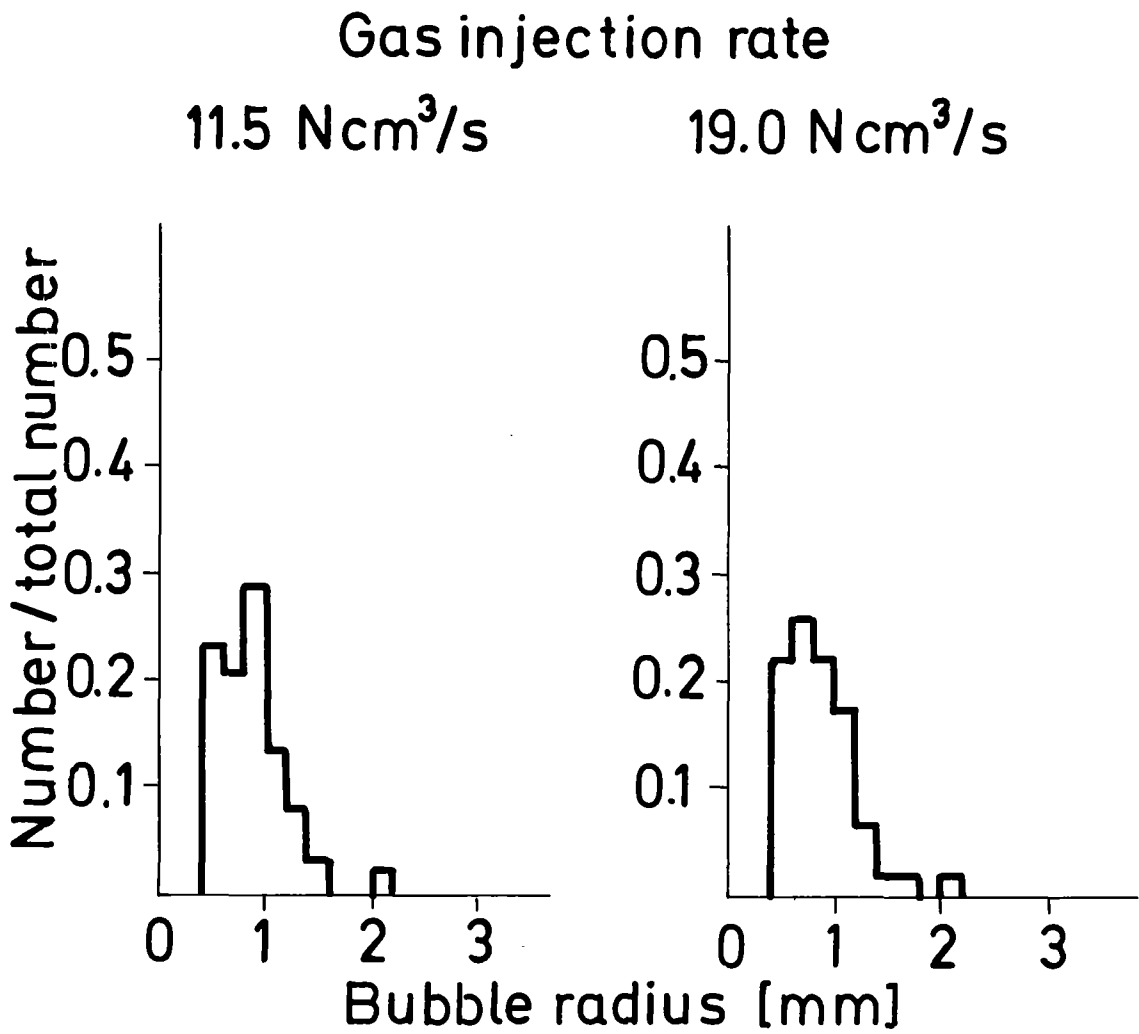


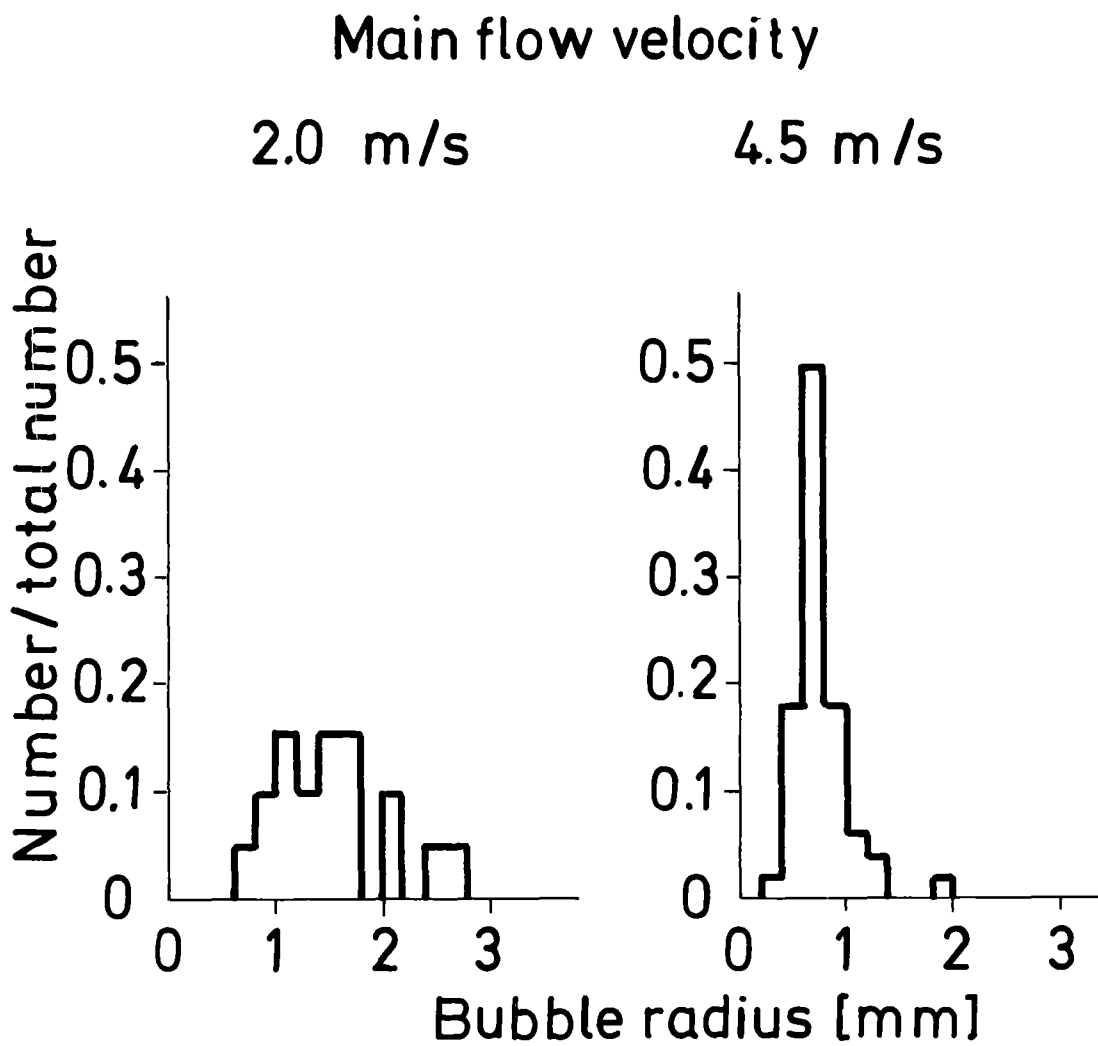
Fig.14 Change of Cavity Size after the Termination of Gas Injection



Downstream gas injection  
Main flow velocity: 3.0 m/s



**Fig.15 Influence of Gas Injection Rate on Bubble Size Spectrum**



Downstream gas injection  
 Gas injection rate:  $11.5 \text{ N cm}^3/\text{s}$



**Fig.16 Influence of Main Flow Velocity on Bubble Size Spectrum**

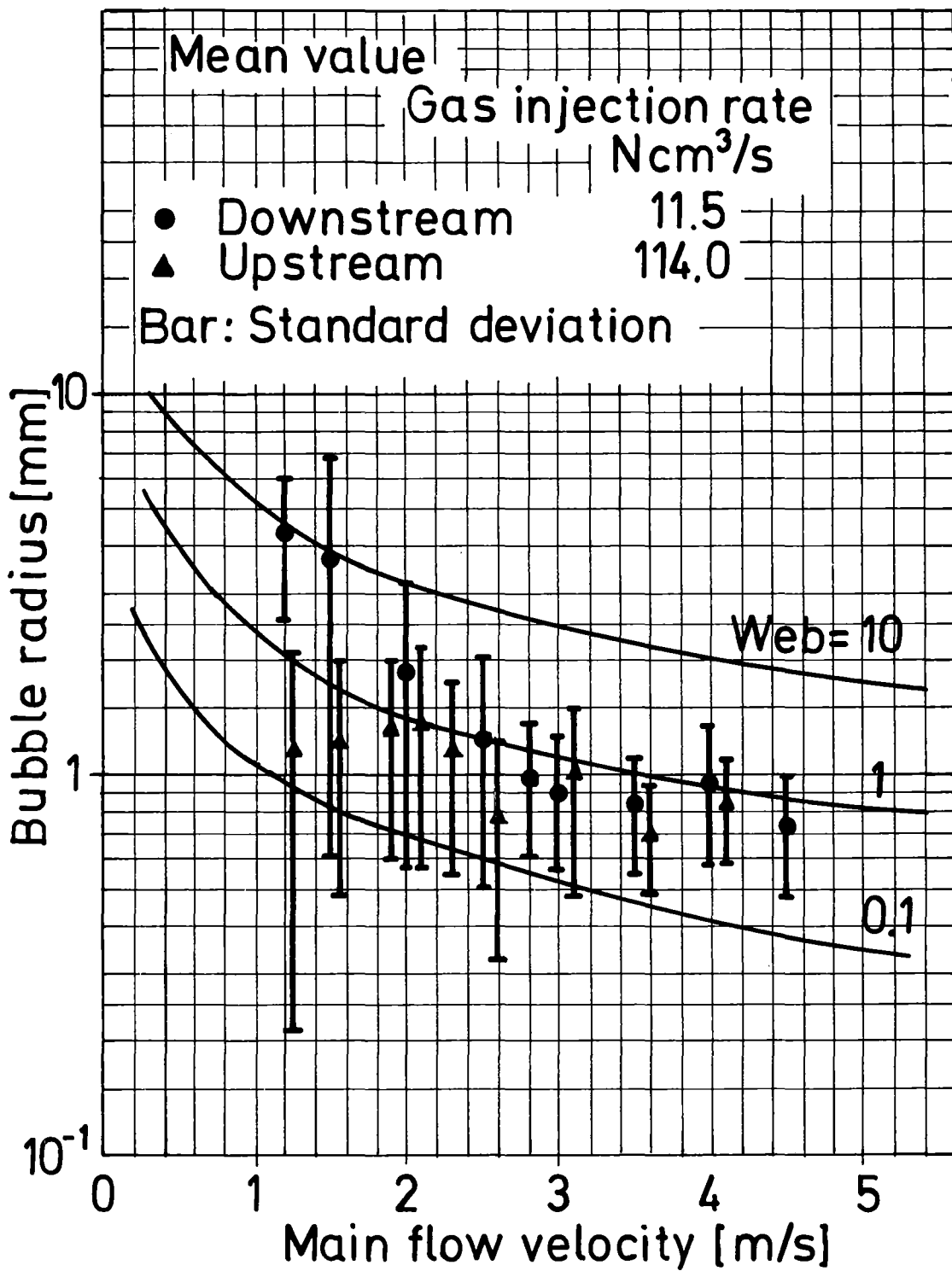


Fig.17 Comparison of the Velocity Dependence of the Size for Different Positions of Gas injection Hole

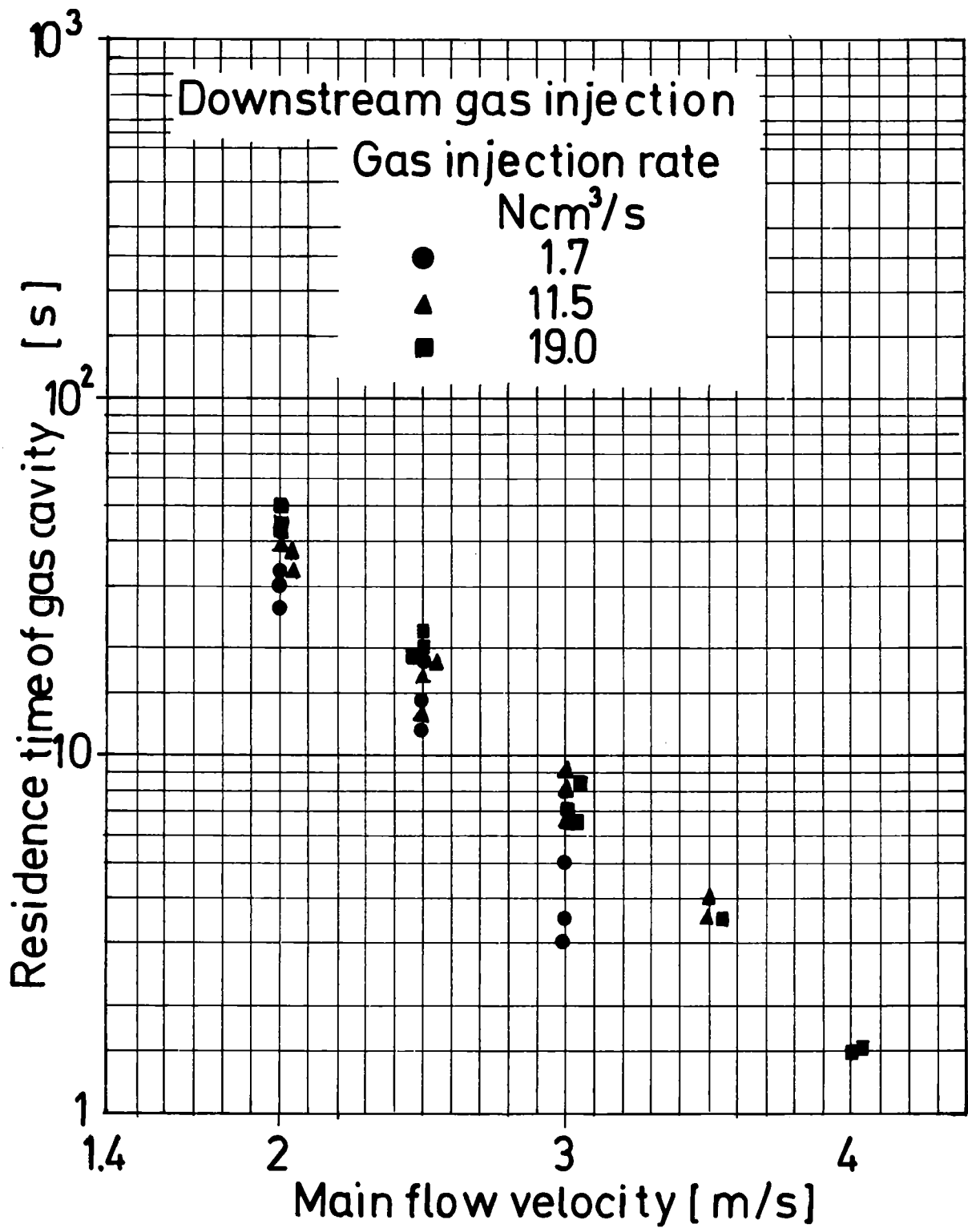


Fig.18 Residence Time of Gas Cavity Versus Main Flow Velocity

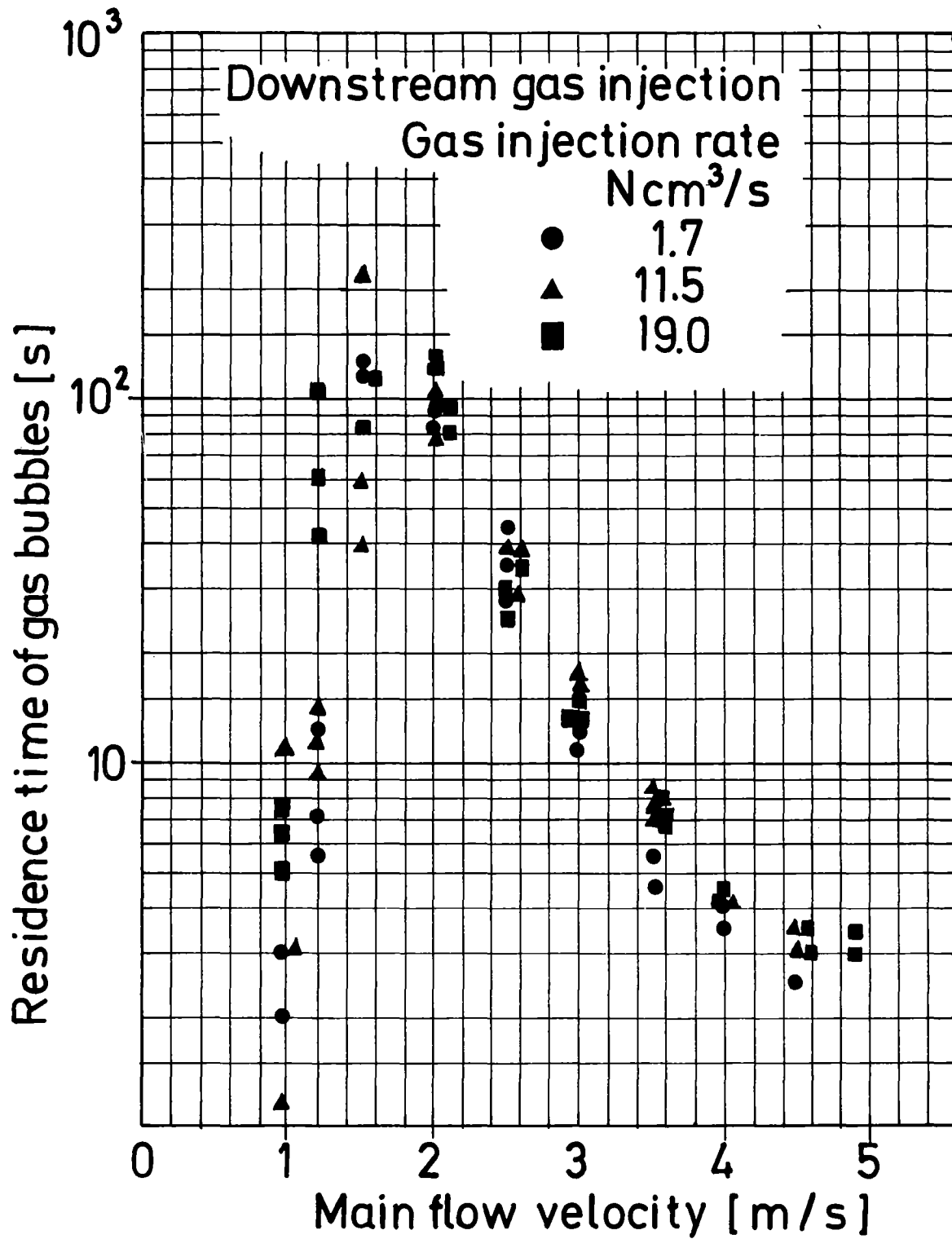


Fig.19 Residence Time of Gas Bubbles Versus Main Flow Velocity